Title

CFD Investigation of Room Ventilation for Improved Operation of a Downdraft Table: Novel Concepts

Journal

Journal of Occupational and Environmental Hygiene, 3(11)

ISSN

1545-9624

Authors

Jayaraman, Buvaneswari
Kristoffersen, Astrid H
Finlayson, Elizabeth U
et al.

Publication Date

2006-11-01

DOI

10.1080/15459620600932551

Peer reviewed

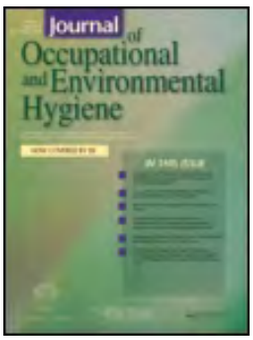

Journal of Occupational and Environmental Hygiene

ISSN: 1545-9624 (Print) 1545-9632 (Online) Journal homepage: https://www.tandfonline.com/loi/uoeh20

CFD Investigation of Room Ventilation for Improved Operation of a Downdraft Table: Novel Concepts

Buvaneswari Jayaraman , Astrid H. Kristoffersen , Elizabeth U. Finlayson & Ashok J. Gadgil

To cite this article: Buvaneswari Jayaraman , Astrid H. Kristoffersen , Elizabeth U. Finlayson & Ashok J. Gadgil (2006) CFD Investigation of Room Ventilation for Improved Operation of a Downdraft Table: Novel Concepts, Journal of Occupational and Environmental Hygiene, 3:11, 583-591, DOI: 10.1080/15459620600932551

To link to this article: https://doi.org/10.1080/15459620600932551

Journal of Occupational and Environmental Hygiene, 3: 583–591
ISSN: 1545-9624 print / 1545-9632 online

DOI: 10.1080/15459620600932551

CFD Investigation of Room Ventilation for Improved Operation of a Downdraft Table: Novel Concepts

Buvaneswari Jayaraman,[1] Astrid H. Kristoffersen,[1,2] Elizabeth U. Finlayson,[1] and Ashok J. Gadgil[1]

[1]Indoor Environment Department, Lawrence Berkeley National Laboratory, Berkeley, California
[2]Norwegian Building Research Institute, Oslo, Norway

We report a computational fluid dynamics (CFD) study of containment of airborne hazardous materials in a ventilated room containing a downdraft table. Specifically, we investigated the containment of hazardous airborne material obtainable under a range of ventilation configurations. The desirable ventilation configuration should ensure excellent containment of the hazardous material released from the workspace above the downdraft table. However, increased airflow raises operation costs, so the airflow should be as low as feasible without compromising containment. The airflow is modeled using Reynolds Averaged Navier Stokes equations with a high Reynolds number k-epsilon turbulence model. CFD predictions are examined for several ventilation configurations. Based on this study, we find that substantial improvements in containment are possible concurrent with reduction in airflow, compared with the existing design of ventilation configuration.

Keywords CFD modeling, contamination control, downdraft table, ventilation

Address correspondence to: Buvaneswari Jayaraman, Indoor Environment Department, Lawrence Berkeley National Laboratory, Berkeley, CA 94720; e-mail:bjayaraman@lbl.gov.

INTRODUCTION

Downdraft tables are used to handle hazardous materials that can become airborne. The ventilation configuration in the room containing the downdraft table affects the downdraft table performance. Experimental work on a downdraft table has been reported;[1] however, no published guidelines are available in the literature for room ventilation design to improve the performance of an industrial downdraft table. Although numerical and experimental work has been published investigating the performance of fume hoods,[2] fume hoods are unsuitable where manipulating operations are required. The present study investigates possible modifications to the ventilation system of a downdraft facility using computational fluid dynamics (CFD). Some of our work on this facility has been reported elsewhere.[3,4]

The objective of this study was to improve containment of the contaminant by changing the ventilation configuration. Energy costs can be reduced if improved containment can be achieved with reduced airflow. The facility under investigation remains contaminated from previous use and is inaccessible for detailed experiments. Therefore, any assessment of improving containment and reducing airflow must be undertaken with simulations. The present study uses CFD to test alternate ventilation and geometric configurations for improved containment of the pollutants.

FACILITY AND MODEL DESCRIPTION

The facility, shown schematically in Figure 1, consists of two rooms connected by a doorway. In the first room, the change room, the worker puts on protective clothing. This room provides an entrance to the second room, the downdraft room (2.3 m × 2.0 m × 2.5 m high), which contains the downdraft table located against the wall opposite to the door. This wall has a pass-through window directly above the downdraft table. After the contaminated packages are passed into the room through this window, the window is closed. As the facility is currently operated, air enters the room through a vertical slot in the door behind the worker and from a rectangular inlet in the ceiling above the table. All airflow exits through the downdraft table. The rooms, constructed in the 1960s, currently have a ventilation configuration that supplies a total of 1700 L/sec (3600 ft^3/min) air to the room. Of this, 1230 L/sec (2600 ft^3/min) are supplied through an opening in the door connecting the two rooms and 470 L/sec (1000 ft^3/min) from the ceiling toward the table. The vertical slot in the door has dimensions of 0.46 m × 0.81 m, with its lower edge located at 10 cm from the floor level. This opening in the door is referred to as the door inlet.

The change room was excluded from the computational domain. When the door is closed, the details of the airflow within the change room were assumed to have no effect on the airflow in the downdraft room. Airflow enters the downdraft room through the door slot, normal to the door, and was treated

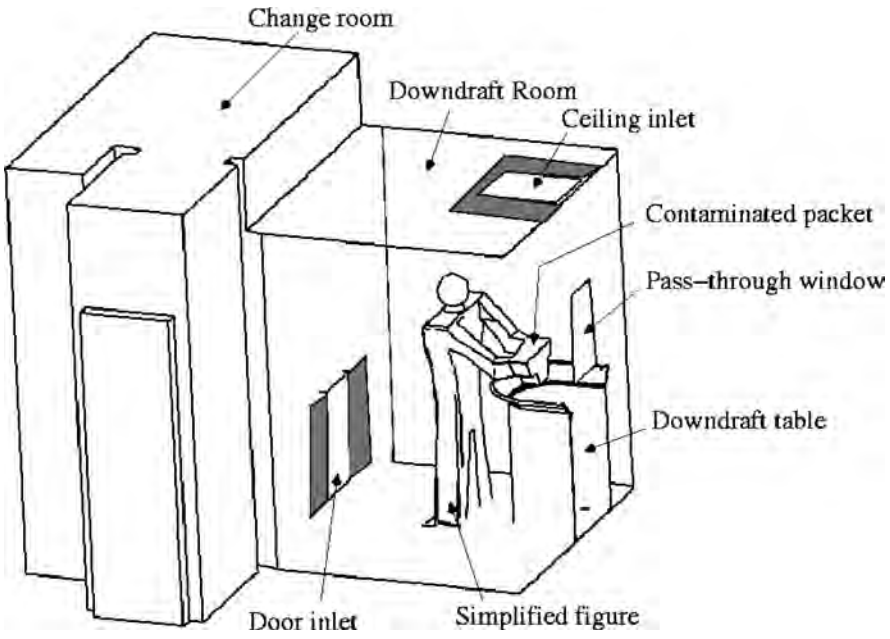

FIGURE 1. Facility geometry including the change room to the left and the downdraft room to the right (2.3 m × 2.0 m × 2.5 m). The geometry includes the downdraft table, simplified worker figure in a protective suit holding the contaminated package, door inlets, pass-through window, and an inlet in the ceiling.

as a boundary condition. The airflow from the inlet in the ceiling was assumed to be straight down and also was treated as a boundary condition. Additional inlets for alternate configurations were all treated as boundary conditions. Inlet boundary conditions had specified flow rates.

A simplified model of a worker simulated the effect of flow blockage by the worker. The worker is assumed to be in a protective suit, and the thermal plume of the worker is neglected (owing to larger than an order of magnitude difference between the plume velocity in still air, and the downdraft room airspeeds). The worker is holding an object representing a contaminated package. The package is held above the downdraft table surface and away from the edge to represent standard working conditions.

Containment for a given velocity field was investigated by first checking the predicted flow paths of massless particles and then, in more detail, checking the predicted concentration of tracer gas. The massless particles and the tracer gas were both released from the package and the two additional locations where worst-case containment was expected: from the rim of the downdraft table, and the perimeter of the (closed) window in the wall behind the downdraft table (Figure 2). Tracks of airborne massless particles give a good indication of whether contaminant will be contained with respect to the mean flow. This is a reasonable minimum criterion to assure containment. Particle tracks can show the effects only of the mean velocity. Additional mixing in the room from turbulent fluctuations can cause increased contamination. To evaluate the additional diffusion caused by turbulence, we simulated a continuous release of a neutrally buoyant tracer gas (as a passive scalar) at the rim of the downdraft tabletop and the perimeter of the pass-through window. Tracer gas has very high diffusivity, much larger than that of particulate contaminants, and represents a maximum criterion for containment of particles.

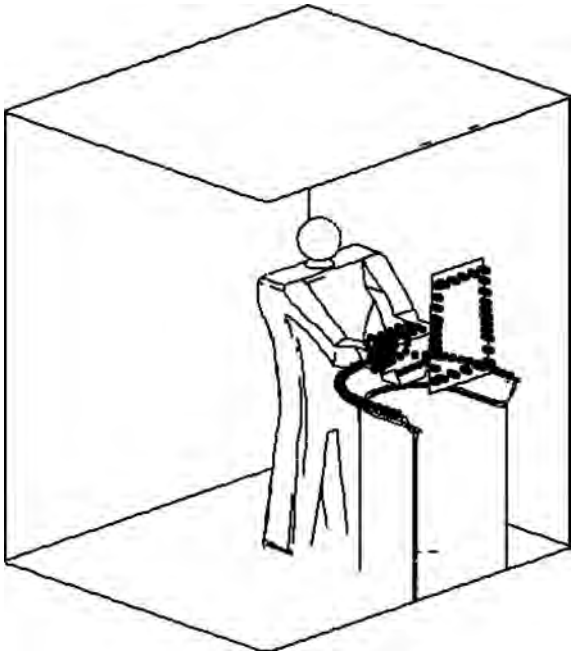

FIGURE 2. Simulated release of massless particles and tracer gas used to determine containment. Release locations are shown as black dots.

We considered several modifications to the existing room operation and geometry by changing the area, location, and airflow from the inlets. One configuration also investigated the performance with a perforated floor as exhaust and perforated ceiling as inlet.

We performed the CFD calculations using the Reynolds averaged form of the Navier Stokes Equations (RANS). The flow is considered incompressible and isothermal with constant air properties. There are several possible choices of turbulence models, none of them perfect. The possible choices are large eddy simulation (LES), realizable k-ε, low Reynolds number k-ε and the standard k-ε models. The LES model actually calculates the turbulent eddies. An LES was not considered because it would have increased the computational and human effort by more than an order of magnitude. Realizable k-ε model was not available as an option in the STAR-CD software (version 3.15; CD-Adapco, New York, N.Y.) used for the present study. The strength of the low Reynolds number k-ε model is that it captures the region of low turbulent Reynolds number that exists close to the wall by integrating the equations all the way to the wall, and it captures the re-laminarization regions in the quiescent part of the flow. As there are no regions of relaminarization in the present case, this model was not used; the standard k-ε turbulence model with wall functions (Eqs. 3 and 4) was used. This model has been used for indoor airflow modeling by other researchers even in the presence of bluff bodies[5] to capture the important features of the flow.

The standard k-ε model also has weaknesses. It is known to have the following two deficiencies: (1) It provides inaccurate prediction of separation points for boundary layers around bluff bodies and overpredicts the turbulent kinetic energy, k, in the stagnation region.[6,7] In the present case the only bluff body is the rim of the downdraft table. The inaccuracies in the prediction of location of separation at the rim of the table will not have a significant effect on the overall prediction of the contamination spill because the flow exits the room through the downdraft table. (2) This model could produce unphysical negative Reynolds stresses around the bluff body that could lead to overprediction of k upstream of the body and underprediction in the near wake region.[8] There is a remedy to this unphysical prediction. The realizable k-ε model that prevents negative values of k can be used to overcome this problem.[9] However, in the current study this model could not be used, as it is not available in STAR-CD.

Finally, we expect that the larger differences (50%) in containment between configurations will not be affected by the choice of a different turbulence model, but the ranking of the configurations with smaller differences (<30%) could be affected.

A finite volume formulation of the following set of equations is solved using STAR-CD software.[5]

$$\frac{\partial U_j}{\partial x_j} = 0 \quad \textbf{(1)}$$

$$U_j \frac{\partial U_i}{\partial x_j} = -\frac{1}{\rho}\frac{\partial P}{\partial x_i} + \frac{\partial}{\partial x_j}\left[\upsilon \frac{\partial U_i}{\partial x_j} - \frac{2}{3}\frac{\partial k}{\partial x_i}\right] \quad \textbf{(2)}$$

$$U_j \frac{\partial k}{\partial x_j} = \frac{\partial}{\partial x_j}\left[\nu \frac{\partial k}{\partial x_j} + \nu_{\text{turb}}\left(\frac{\partial U_i}{\partial x_j} + \frac{\partial U_j}{\partial x_i}\right)\frac{\partial U_i}{\partial x_j}\right] - \varepsilon \quad \textbf{(3)}$$

$$U_j \frac{\partial \varepsilon}{\partial x_j} = \frac{\partial}{\partial x_j}\left[\left(\upsilon_{\text{molec}} + \frac{\upsilon_{\text{turb}}}{1.22}\frac{\partial \varepsilon}{\partial x_j}\right)\right] + \frac{\varepsilon}{k}\left[1.44\upsilon_{\text{turb}}\left(\frac{\partial U_i}{\partial x_j} + \frac{\partial U_j}{\partial x_i}\right)\frac{\partial U_i}{\partial x_j}\right] - 1.92\frac{\varepsilon^2}{k} \quad \textbf{(4)}$$

$$U_j \frac{\partial C}{\partial x_j} = \frac{\partial}{\partial x_j}\left[\left(D_{\text{molec}} + \frac{\upsilon_{\text{turb}}}{\sigma_m}\right)\frac{\partial C}{\partial x_j}\right] \quad \textbf{(5)}$$

where P is the pressure; ρ is the density; U_i are the mean velocity components; x_i are rectilinear orthogonal coordinates; k is the turbulent kinetic energy; ε is the dissipation rate of k; C is the tracer concentration, $\nu = \nu_{\text{turb}} + \nu_{\text{molec}}$ where ν_{molec} is the molecular kinematic viscosity and ν_{turb} is the turbulent kinematic viscosity: $\nu_{\text{turb}} = 0.09k^2\varepsilon^{-1}$. D_{molec} is the molecular diffusivity of air in air and σ_m is the turbulent Schmidt number, assigned a value of 0.6.

Our recent research[10] shows that a RANS model with a second-order differencing scheme that suppresses numerical diffusion can provide acceptable (i.e., within a factor of two compared with experimental measurements) detailed predictions for pollutant dispersion. Justification for our current approach rests on the successful CFD comparison with a previous experiment.[10]

Equations for the airflow were first solved to obtain a steady-state velocity field in the downdraft room using the SIMPLE algorithm,[11] and a second-order differencing scheme. The tracer gas transport equation was solved by taking this airflow field as given and treating the tracer gas as a neutrally buoyant and nonreacting scalar. Examination of the simulated tracer gas concentration throughout the downdraft room gave an indication of the spread of the tracer gas due to turbulent diffusion. Mass conservation of the air is fulfilled by specifying, as boundary conditions, that same amount of air enters the room leaves the room. Following Sorensen and Nielsen,[12] a grid refinement study was carried out by locally refining the grid in regions of higher velocity and pressure gradients resulting in a grid convergence index of 0.08. All the simulations presented in this study were carried out using the fine grid with 670,000 nodes.

The steady-state airflow calculations were terminated when the normalized sum of the residuals decrease to less than 1.0e–4. The tracer dispersion was calculated for this airflow field. The calculations for the steady-state solution of the tracer were terminated when the normalized sum of the residual became less than 5.0e–5. The mass conservation of tracer gas was checked and found to be within 1% for all simulated cases.

Because the tracer gas responds to the turbulent diffusion just as much as air, its release provides an estimate of dispersion and containment of species with high diffusivity. Particles have lower diffusivity than tracer gas, so particles released at the same locations and with the same velocity will diffuse less and thus can be expected to be better contained than tracer gas.

Particles can be released with an initial velocity owing to a small amount of mechanical energy being imparted to them. In that case, the particles will initiate their travel with some momentum and may not follow the streamlines. We demonstrate below that this is not a cause for concern.

Mechanically generated powder constituents are typically larger than about 10 μm. For a given launch velocity, larger particles travel farther before coming to momentum equilibrium with the surrounding air. The time for reaching equilibrium is called the relaxation time.

Consider a 100-μm particle released from the contaminated packet 4 inches from the rim of the downdraft table, toward the rim. The relaxation time for a 100 μm particle is 3.1×10^{-2} sec.[13] A launch velocity of more than 3.2 m/sec (630 ft/min) would be required for the particle to reach the rim. For a 10-μm particle, the velocity would be two orders of magnitude higher. Because the downdraft table is not used for explosive releases, we do not anticipate particles leaving the package at velocities high enough to reach the rim.

Figures 3 and 4 show the section planes that will be used to display the results.

We now introduce a measure of the contamination spill, S, in the room. The spill is calculated throughout the computational domain excluding the cells inside the downdraft table and the cells where the tracer gas is released. For a small release rate of tracer, the spill was defined as the integral of the tracer-concentration-weighted cell volumes divided by the same volume, normalized by the concentration at the exhaust. If the release rate of tracer is X kg/sec and the fresh air supply rate is M kg/sec and $X \ll M$, then we can write

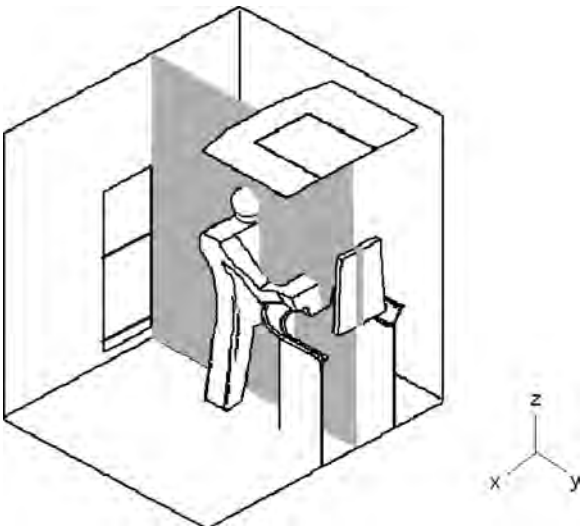

FIGURE 3. The Y-Z section used for displaying results in subsequent figures. The plane passes through the middle of the human figure showing the asymmetry of the downdraft table position within the room. Center plane of downdraft table is 33 inches(0.84 m) from the left wall and 56 inches (1.42 m) from the right wall. This section illustrates the containment in front of the worker and around the package. Note that the display plane cuts through the torso of the figure and misses both legs; hence, legs appear missing in this view in Figures 6–9.

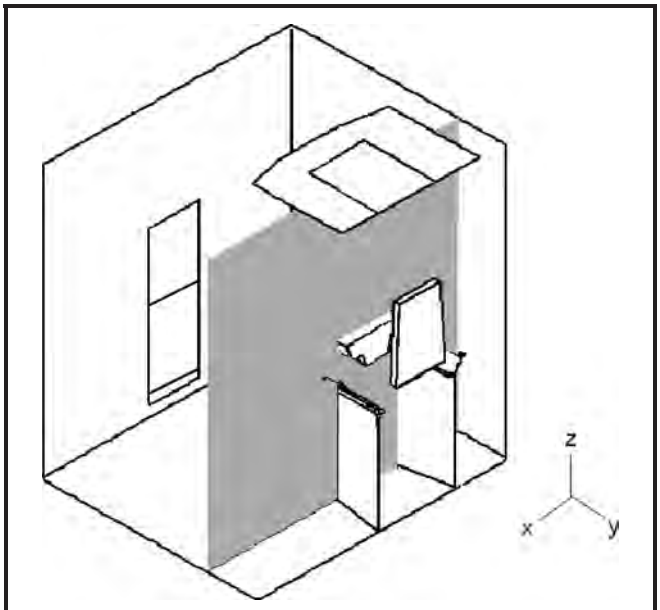

FIGURE 4. The X-Z section used for displaying results in subsequent figures. The plane cuts through the middle of the contaminated package. This view shows how the contamination is spread into the room on either side of the table.

$$S = \frac{\int CdV}{\int dV}\frac{M}{X} \qquad \textbf{(6)}$$

Mass balance requires that the concentration at the exhaust must be $X/(X + M)$ at steady-state. In an instantaneously perfectly mixed room, the tracer gas concentration in the room will be the same as the concentration at the exhaust. Therefore, for an instantaneously perfectly mixed room $C = X/(X+M)$. When $X \ll M$, then $C = X/M$ and the spill measure $S = X/M * M/X = 1$. If the contaminants are fully contained into the downdraft table $S = 0$, and there is no spill. The spill measure gives a measure of the average concentration of the tracer in the room, in the steady-state and is normalized to be between 1 (max) and 0 (min). So, for a given spill measure, S, the average pollutant concentration in the downdraft room, outside the downdraft table, is obtained by multiplying the exhaust concentration of the pollutant by the spill measure.

Average concentration of pollutant in the downdraft room=

$$S^*\frac{X}{M} \qquad \textbf{(7)}$$

Description of the Different Configurations

The description of the different geometries is shown in Table I.

The existing ceiling inlet is shown in Figure 1 as the non-shaded inlet in the ceiling (51 cm wide and 64 cm long). The large ceiling inlet includes the shaded area in the ceiling in

TABLE I. Definitions of Inlet Geometries

Inlet Type	Description	Area m^2(in^2)
Ceiling inlet	Existing	0.32 (500)
	Large	1.07 (1659)
	Perforated	4.42 (6843)
Door inlet	Existing	0.37 (576)
	Large	0.59 (911)
Side	Left	0.65 (1000)
	Right	0.65 (1000)
Airvest		0.17 (260)

TABLE II. Summary of Different Geometry Configurations Investigated

Configurations	Inlet Ceiling	Inlet Door	Outlet Floor	Airvest	Flow Side
A	Existing	Existing	None	None	None
B	Large	Existing	None	None	None
C	Large	Large	None	None	None
D	Perforated	None	Perforated	None	None
E	Existing	Existing	None	Yes	Right and left

Figure 1 (125 cm wide, and 86 cm long). The perforated ceiling inlet assumes that the entire ceiling is a perforated plate and acts as an inlet. The perforated ceiling inlet is modeled with a perforated full-floor exhaust. The existing door inlet is shown as the nonshaded inlet behind the worker (46 cm wide and 81 cm high). The large door inlet includes the shaded area on the left and right sides of the existing door inlet (72 cm wide and 81 cm high). If one draws a vertical plane similar to the one identified on Figure 3, the left edge of the large door inlet behind the worker will be coplanar with the left edge of the large ceiling inlet. The side inlets are positioned on the walls on the left and right sides of the downdraft table. The left inlet is on the left-hand side wall of the worker, and the right inlet on the right-hand side wall of the worker. The low edge of the side inlets are 77 cm from the floor level; each inlet is 1 m long and 65 cm high, and its vertical edge nearest to the wall with the pass-through window is 30 cm from that wall.

The airvest is a device that can be worn by the worker, covering the worker's chest. The airvest can also be positioned in front of the downdraft table at the height of the worker's chest. The worker should then position himself behind the airvest when opening the packet. Previous research by Gadgil and colleagues reported on reducing worker exposure using an airvest.[14]

Table II lists the different geometrical configurations.

RESULTS

Discussion of Existing Configuration

As a first step we explored the containment capability of the existing configuration (Configuration A) as it is currently operating; 470 L/sec (1000 ft^3/min) downward from the ceiling inlet and 1230 L/sec (2600 ft^3/min) through the door.

Figure 5 shows the tracer concentration contours and velocity pattern for the existing configuration. All concentration contours presented herein are in log scale. In the y-z view, the spilled tracer touches the worker's chest and spreads into the room. In the x-z view, the tracer is spread on both sides of

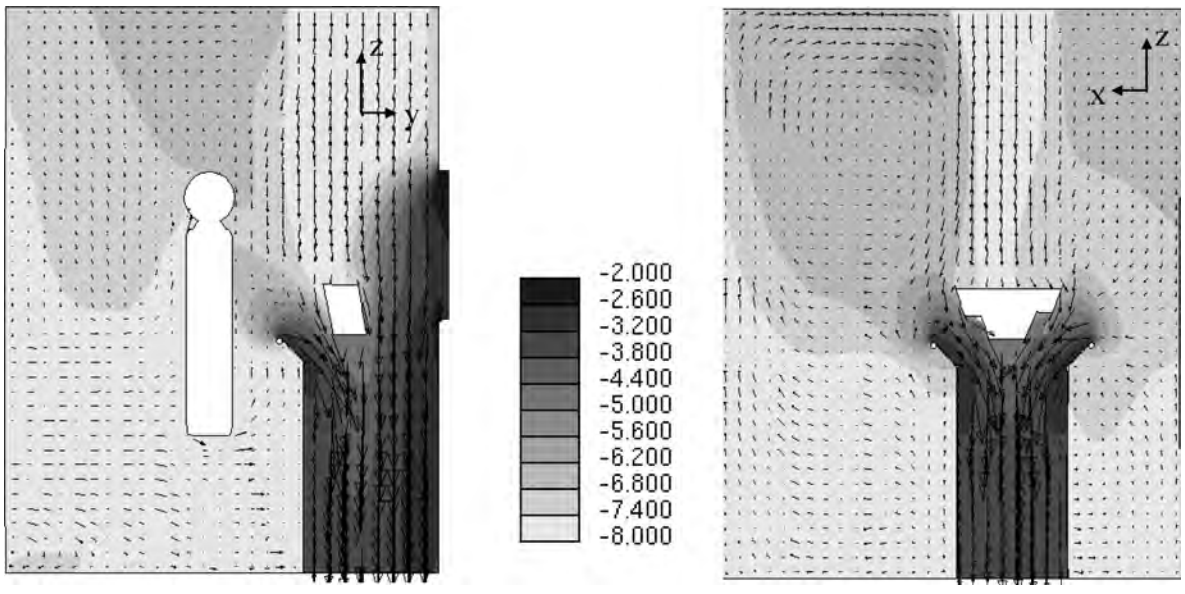

FIGURE 5. Tracer gas concentration (log of normalized concentration) and velocity of existing geometry with currently operated airflow rates: 470 L/sec (1000 ft^3/min) from the ceiling inlet and 1220 L/sec (2600 ft^3/min) from the door inlet, when releasing 1 g/sec of tracer into the room.

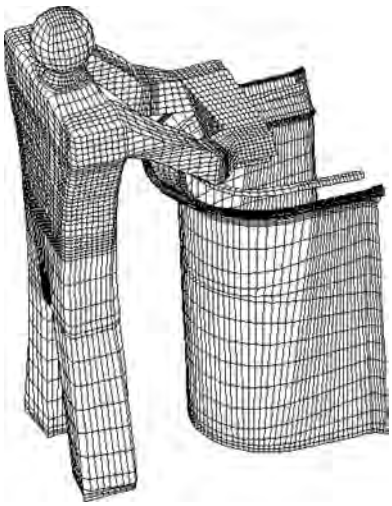

FIGURE 6. Tracer gas release locations 10 cm from the table rim, in the plane of the table rim.

the table. A recirculating airflow pattern can be seen on the left-hand side of the table in the x-z view. The airflow from the door inlet encounters either the lower part of the downdraft table or the opposite wall. The part of the airflow that rises along the wall (not seen in Figure 6) produces a recirculating flow in the room. The tracer reaches this recirculating pattern by turbulent diffusion and becomes effectively spread in the room by following the mean flow recirculation. The contamination spill for the existing configuration was found to be $S = 8.64 \cdot 10^{-4}$.

The containment of the tracer gas is significantly increased when releasing tracer gas inside the downdraft table rather than releasing it from the rim and around the pass-through window (Figure 6). The spill measure for this release was measured to $S = 0.75 \cdot 10^{-4}$. It is recommended that the packet be opened inside a ring 10 cm from the downdraft table rim.

The existing configuration produced a recirculating pattern on the left-hand side of the table in the x-z view. Eighteen different simulations with the same configuration but with reduced airflow were performed, varying the airflow from the ceiling inlet from 190 to 470 L/sec (400 to 1000 ft^3/min) and varying the airflow from the door inlet from 190 to 1220 L/sec (400 to 2600 ft^3/min). Results from previous work on this facility show that decreasing the airflow with the same geometry as the existing setup will reduce the contamination of the room.[3] The smallest spill measure among these 18 simulations was found for airflow from the ceiling inlet 380 L/sec (800 ft^3/min) and airflow from the door inlet 760 L/sec (1600 ft^3/min). The tracer concentration for configuration A with the "best" reduced airflow settings was found at 380 L/sec (800 ft^3/min) from the ceiling inlet and 760 L/sec (1600 ft^3/min) from the door inlet. The spill measure was calculated to $S = 4.36 \cdot 10^{-4}$, a reduction of 50% compared with the existing airflows. The spill is still high because of the recirculating pattern that is still present. We now want to investigate other configurations to see if the recirculating pattern can be suppressed and, hence, further reduce the spill measure.

ALTERNATE CONFIGURATIONS

Configuration B has an enlarged ceiling inlet and existing door inlet. Nineteen different runs varying the airflow at the inlets were performed. The case with the lowest spill measure has airflow from the ceiling inlet of 470 L/sec (1000 ft^3/min) and from the door inlet 380 L/sec (800 ft^3/min). The enlarged ceiling inlet reduces the extent of the recirculating flow seen in the x-z view of the velocity. This case further reduces the spill by about a factor of two giving a spill measure of $S = 2.42 \cdot 10^{-4}$. The tracer escapes from the downdraft table and enters the recirculating flow, contaminating the left side of the downdraft table.

Configuration C has the same ceiling inlet as Configuration B but also has an enlarged door inlet. The velocity and tracer concentration is shown in Figure 7. Configuration C suppresses the recirculating flow further but is still present. The spill measure is further slightly reduced to $S = 2.22 \cdot 10^{-4}$.

Configuration D is successful in suppressing the recirculating pattern on the left side of the downdraft table. Airflow of 800 L/sec (1700 ft^3/min) is injected uniformly from the ceiling, resulting in vertically downward airflow from the ceiling. Part of the air leaves the room through a perforated floor; the rest leaves through the downdraft table. Three simulations with this configuration were performed, with 10%, 20%, and 30% of the flow leaving the room through the perforated floor. Part of the airflow from the ceiling directly enters the downdraft table, whereas the rest proceeds toward the floor, mostly beside and behind the worker. A part of this airflow exits the room through the perforated floor, but the rest rises in front of the worker and is drawn into the downdraft table. Very low velocities ($\sim$0.1 m/sec) result in the region in front of the worker where the rising air meets the downward airflow from the ceiling. The tracer gas transported by turbulent diffusion into this region contaminates the area around the downdraft table and in front of the worker. Forcing a larger part of the air to exhaust through the floor would prevent the air from rising when hitting the floor.

Due to the size and geometry of this room, about 70% of supplied air must exhaust through the floor to prevent the airflow from rising in front of the worker. The average air speed at the downdraft table face must exceed the recommended value of 200 ft/min,[15] so the minimum acceptable flow to exit through the downdraft table is 560 L/sec (1200 ft^3/min). Having 560 L/sec (1200 ft^3/min) leaving the room through the downdraft table, and 70% of the injected air leaving the room through the floor, means that a total airflow of about 1880 L/sec (4000 ft^3/min) must be injected from the perforated ceiling. A total airflow of 1880 L/sec (4000 ft^3/min) is considered too high, so a different configuration is more appropriate.

Configuration E has a ceiling inlet and a door flow inlet (as the original case) but adds three others. The airvest blows low-velocity air horizontally toward the downdraft table away from

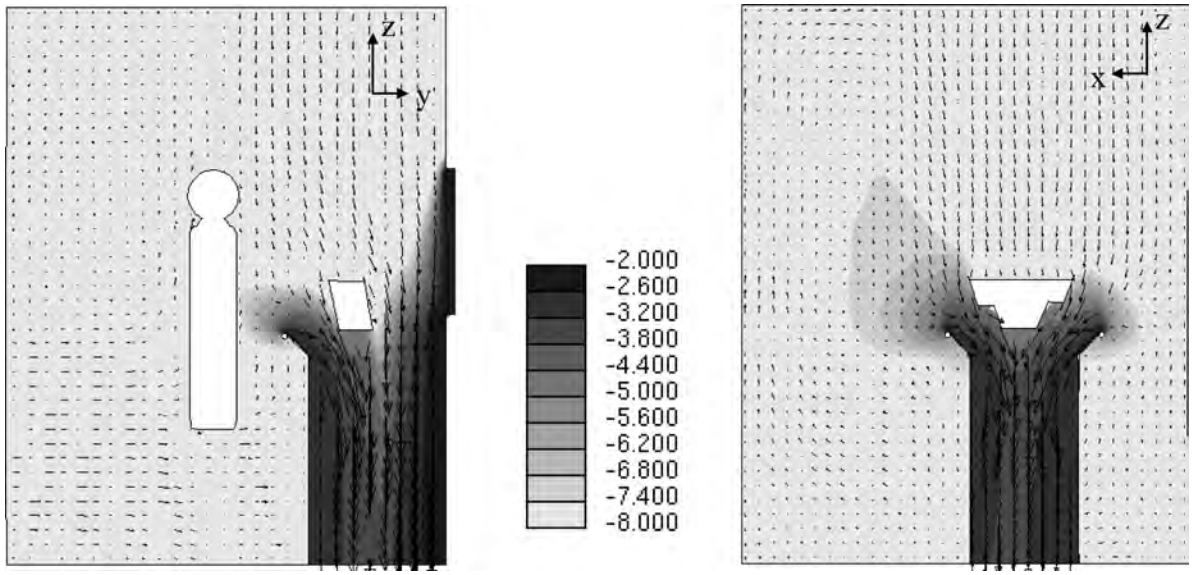

FIGURE 7. Velocity and tracer concentration (log of normalized concentration) with release of 1 g/sec of tracer, Configuration C with operating airflow rates: 470 L/sec (1000 ft^3/min) from the ceiling inlet and 470 L/sec (1000 ft^3/min) from the door inlet.

the body,[15] which prevents contaminated air from diffusing into the worker's breathing zone. In addition, two large-area, low-velocity side inlets are positioned at either side of the downdraft table. The low-velocity airflow from these side inlets results in a slow, steady flow toward the downdraft table with low turbulent kinetic energy. The airflows from the different inlets are adjusted, so the released particles are contained within the downdraft table and not spread into the room. The best (optimal) airflow rates were found to be: 70 L/sec (150 ft^3/min) from the airvest, 380 L/sec (800 ft^3/min) from the ceiling inlet, 280 L/sec (600 ft^3/min) from the door inlet, 380 L/sec (800 ft^3/m) from the left side inlet, and 140 L/sec (300 ft^3/min) from the right side inlet. Fifteen different runs varying the airflow rates were performed with this configuration. A slow flow toward the downdraft table from inlets surrounding the downdraft table leads to increased containment.

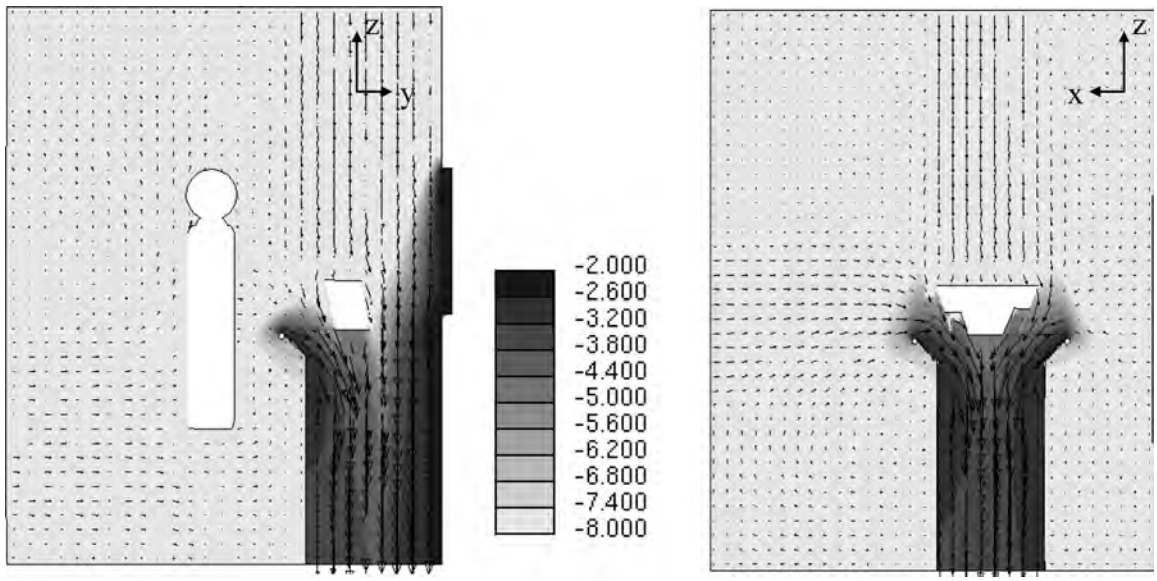

FIGURE 8. Velocity and tracer concentration (log of normalized concentration) with release of 1 g/s of tracer, Configuration E with operating airflow rates: 380 L/sec (800 ft^3/min) from the ceiling inlet, 280 L/sec (600 ft^3/min) from the door inlet, 70 L/sec (150 ft^3/min) from the airvest, 380 L/sec (800 ft^3/min) from the left side inlet and 140 L/sec (300 ft^3/min) from the right side inlet.

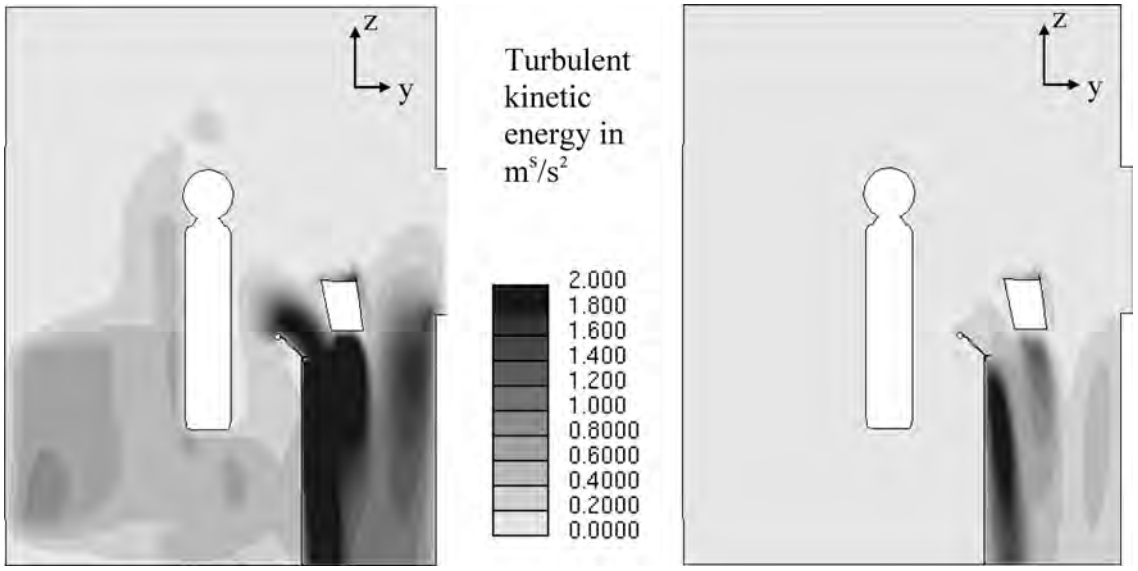

FIGURE 9. Turbulent kinetic energy for existing case (left) and for configuration E (right). Note dramatically lower turbulent kinetic energy throughout the room in Configuration E, which aids in improved containment.

A few simulations were also performed with narrower side inlets. These simulations predicted significant spill. Only when the side inlets had large area and the airflow velocities small, could we see a significant reduction in the spill measure. The spill measure is reduced from $S = 8.64 \cdot 10^{-4}$ for the existing case to $S = 1.58 \cdot 10^{-4}$ for Configuration E, a reduction of 82%. The airflow is reduced by 26%. The tracer concentration and velocities for Configuration E can be seen in Figure 8. The turbulent energy is also low for this configuration, as seen in Figure 9. The turbulent intensity is highest in the room at the rim of the table. The high turbulent intensity at the rim leads to high turbulent diffusivity, which leads to diffusive escape of some amount (though small) of the tracer gas from the rim into the room.

A simulation adding the airvest (without side inlets) to Configuration A was also performed (not reported). This resulted in approximately the same result as Configuration A, except that the area between the worker and the downdraft table was not contaminated due to the injection of fresh air from the airvest. Thus, the worker's exposure would indeed be reduced without noticeably reducing the spill measure.

The tracer concentration for a release of tracer gas from 10 cm inward from the downdraft table rim for Configuration E resulted in a spill measure of $S = 0.59 \cdot 10^{-4}$, a reduction of 21% compared with the existing configuration. Opening the packet inside a ring of 10 cm inside the downdraft table is highly recommended.

The best run (based on calculation of the spill measure) of each configuration is listed in Table III. The breathing zone concentration calculated in a volume of 1 ft^3 adjacent to and below the nose level of the worker is listed in Table IV. Configurations A–D have slightly higher breathing zone concentrations than the existing configuration because these modified configurations have lower velocity flow coming in from the ceiling inlet. The addition of low-velocity air from the airvest of the worker in Configuration E eliminates the accumulation

TABLE III. Spill Measure for the Existing and Best Case for Each Configuration

Configuration	Ceiling Inlet L/sec (ft^3/min)	Door Inlet L/sec (ft^3/min)	Floor outlet L/sec (ft^3/min)	Airvest L/sec (ft^3/min)	Left Side Inlet L/sec (ft^3/min)	Right Side Inlet L/sec (ft^3/min)	Total Airflow L/sec (ft^3/min)	Spill Measure 10^{-4}
Existing	470 (1000)	1220 (2600)	N/A	N/A	N/A	N/A	1690 (3600)	8.64
A	380 (800)	760 (1600)	N/A	N/A	N/A	N/A	1140 (2400)	4.36
B	470 (1000)	380 (800)	N/A	N/A	N/A	N/A	850 (1800)	2.42
C	470 (1000)	470 (1000)	N/A	N/A	N/A	N/A	940 (2000)	2.22
D	800 (1700)	None	240 (510)	N/A	N/A	N/A	800 (1700)	2.32
E	380 (800)	280 (600)	N/A	70 (150)	380 (800)	140 (300)	1250 (2650)	1.58

TABLE IV. Breathing Zone Concentration for the Existing and Best Case for Each Configuration

Configuration	Breathing Zone Concentration 10^{-5}
Existing	0.22
A	0.35
B	0.3
C	0.27
D	0.34
E	0.056

of the contaminant in front of the worker and results in the lowest breathing zone concentration.

CONCLUSION

Despite the industrial wide-scale use of downdraft tables, published literature does not provide guidelines or measures of how well a downdraft table performs under specific ventilation configurations in a room.

This article defines a dimensionless "spill measure" that provides a quantitative measure of pollutant containment for a downdraft table operated under specific ventilation conditions. The spill measure has a maximum possible value of 1 and a minimum possible value of 0. In the steady-state, the average concentration of the pollutant in the room is given by multiplying spill measure by the pollutant concentration in the exhaust from the room (or by weighted average pollutant concentration in the exhaust, if the room has multiple exhausts).

We examined the downdraft table performance using CFD simulations, verified with an earlier published comparison with different experiments. We showed that reducing the airflow supply in the existing geometric configuration would reduce the spill measure and even the concentration of pollutant in the room (the reduction in the spill measure is larger than the increase in the pollutant concentration in the exhaust arising from reduction in the fresh air supply to the room). We also showed that even more reduction in the spill measure, and improved containment, is possible by increasing the area of inlets in the ceiling and the door with appropriate changes in the respective airflow supply rates, or with using a perforated ceiling air supply and a perforated floor exhaust. Finally, we showed that using two, side-wall-mounted air supplies and an airvest, the spill measure could be reduced even further, by more than a factor of 5 compared with the original configuration, thus saving conditioning energy for the air supply (26%) and concurrently improving the containment of the contaminant and, hence, worker protection (82%).

ACKNOWLEDGMENTS

This work was partly supported by the Norwegian Research Council through the Strategic Institute Program at the Norwegian Building Research Institute, and the Lawrence Livermore National Laboratory.

REFERENCES

1. **Spencer, A.B., C.F. Estill, J.B. McCammon, R.L. Mickelsen, and O.E. Johnston:** Control of ethyl methacrylate exposures during the application of artificial fingernails. *Am. Ind. Hyg. Assoc. 58*:214–218 (1997).
2. **Lan, N.S., and S. Viswanathan:** Numerical simulation of airflow around a variable volume/constant face velocity fume cupboard. *Am. Ind. Hyg. Assoc. 62*:303–331 (2001).
3. **Lawrence Berkeley National Laboratory (LBNL):** *CFD Analysis of LLNL Downdraft Table* by E.U. Finlayson, B. Jayaraman, A.R. Kristoffersen, and A.J. Gadgil (Report No. LBNL-53883). Berkeley, Calif.: LBNL, 2003.
4. **Lawrence Berkeley National Laboratory (LBNL):** *Investigation of Room Ventilation for Improved Operation of a Downdraft Table* by B. Jayaraman, A.R. Kristoffersen, E.U. Finlayson, and A.J. Gadgil (Report No. LBNL-55561). Berkeley, Calif.: LBNL, 2004.
5. **Brohus, H., and P.V. Nielsen:** CFD models of persons evaluated by full-scale wind channel experiments. In *Proceedings of ROOMVENT '96, 05th International Conference on Air Distribution in Rooms*, Yokohoma, Japan, July 17–19, 1996. Vol. 2, pp. 137–144.
6. **Rodi, W.:** On the simulation of turbulent flow past bluff bodies. *J. Wind Eng. Ind. Aerodyn. 46–47*:3–19 (1993).
7. **Rodi, W.:** Comparison of LES and RANS calculations of the flow around bluff bodies. *J. Wind Eng. Ind. Aerodyn.* 69–71:55–75 (1997).
8. **Bosch, G., and W. Rodi:** Simulation of vortex shedding past a square cylinder with different turbulence models. *Int. J. Num. Methods Fluids* 28:601–616 (1998).
9. **Shih, T., W.W. Liou, A. Shabbir, Z. Yang, and J. Zhu:** A new k-ε eddy viscosity model for high Reynolds number turbulent flows. *Comput. Fluids 24*:227–238 (1995).
10. **Finlayson, E.U., A.J. Gadgil, T.L. Thatcher, and R.G. Sextro:** Pollutant dispersion in a large indoor space: Computational fluid dynamics (CFD) predictions and comparison with a scale model experiment for isothermal flow. *Indoor Air 14(4)*:272–283 (2004).
11. **Patankar, S.V.:** *Numerical Heat Transfer and Fluid Flow*. Washington D.C.: Hemisphere, 1980. pp. 126–131.
12. **Sorensen, D.N., and P.V. Nielsen:** Quality control of computational fluid dynamics in indoor environments. *Indoor Air 13*:2–17 (2003).
13. **Hinds, W.C.:** *Aerosol Technology: Properties, Behavior, and Measurement of Airborne Particles.* New York: John Wiley & Sons, 1999. pp. 112–113.
14. **Lawrence Berkeley National Laboratory (LBNL):** *Reduced Worker Exposure and Improved Energy Efficiency in Industrial Fume Hoods Using an Airvest,* by A.J. Gadgil, D. Faulkner, and W.J. Fisk (LBNL-32244). Berkeley, Calif.: LBNL, 1992.
15. **American Conference of Governmental Industrial Hygienists (ACGIHR):** *Industrial Ventilation. A Manual of Recommended Practice 22nd Edition*. Cincinnati, Ohio: ACGIH, 1995.